

Net Toroidal Magnetic Moment in the Ground State of a {Dy₆}-Triethanolamine Ring

Liviu Ungur,^{*,‡} Stuart K. Langley,[†] Thomas N. Hooper,[§] Boujemaa Moubaraki,[†] Euan K. Brechin,[§] Keith S. Murray,[†] and Liviu F. Chibotaru^{*,‡}

[‡]Division of Quantum and Physical Chemistry and INPAC—Institute of Nanoscale Physics and Chemistry, Celestijnenlaan 200F, Katholieke Universiteit Leuven, B-3001 Leuven, Belgium

[†]School of Chemistry, Monash University, Building 23, Clayton, Victoria 3800, Australia

[§]EaStCHEM School of Chemistry, University of Edinburgh, West Mains Road, Edinburgh, U.K. EH9 3JJ

Supporting Information

ABSTRACT: A toroidal magnetic moment in the absence of conventional total magnetic moment is observed in a {Dy₆} ring. The reason for the net toroidal arrangement of the local magnetic moments is the high symmetry of the complex in combination with strong intra-molecular dipolar interactions between Dy ions. The description of single-ion and inter-ion anisotropic magnetic interactions is achieved here for the first time fully *ab initio*, i.e., without use of phenomenological parameters.

The non-collinear arrangement of the magnetic moments of individual magnetic centers in polynuclear molecular magnets can result in fascinating magnetic behavior.¹ Among various possibilities for this arrangement, the toroidal magnetic state seems to be most promising for future applications in quantum computing and information storage.² A key property of toroidal magnetic moments is their insensitivity to homogeneous magnetic fields.^{2a} This means that the two components of the toroidal magnetic state, corresponding to circular arrangements of magnetic moments in opposite directions,^{1a} will be much more protected against the action of a magnetic field, compared to the spin projection eigenstates of a true spin $S = 1/2$.³ Moreover, since the magnetic field produced by a net toroidal moment decays much faster than the field of a normal magnetic dipole, qubits designed on the basis of toroidal moments will be much less interfering and, therefore, could be packed much more densely than spin qubits.³ Finally, the toroidal magnetic moment interacts with a dc current passing through the molecule⁴ or a time-varying electric field⁵ via magneto-electric coupling,⁶ and this allows the moment to be controlled and manipulated purely by electrical means, a property much sought-after for molecular devices. The latter is a great advantage over collinear spin complexes, which can only be controlled by an applied magnetic field.

The toroidal arrangement of local magnetic moments has been found recently in lanthanide magnetochemistry and was first discovered in Dy₃ triangles.^{1a} These toroidal states proved to be quite robust: they remained almost unchanged upon polymerization, resulting in {Dy₃Cu} chains.⁷ The non-magnetic toroidal state was also very recently observed in {Dy₄} tetramers.⁸ Herein we report a theoretical study of the

six-membered wheel [Dy(Htea)(NO₃)₆·8MeOH (H₃tea = triethanolamine), recently synthesized and characterized,⁹ and show that it also exhibits a toroidal moment in the ground state. However, in contrast to all known previous compounds, this {Dy₆} complex owes its net toroidal magnetic moment to high rotational symmetry.

Ab initio calculations were performed for the mononuclear Dy fragments of the Dy₆ compound using the experimental structure.⁹ Due to the S_6 symmetry of the complex, all Dy centers are electronically equivalent, and therefore, it was sufficient to consider one single Dy center. For fragment calculations we have employed two structural approximations, A (small) and B (large) shown in Figures S1 and S2. For each calculated fragment we have employed two basis set approximations, 1 (small) and 2 (large), resulting in four computational approximations, A1, A2, B1, and B2 (Table S1). The necessity to consider two structural approximations and two basis set approximations is dictated by the need to check the convergence of the results of calculations with respect to the size of the calculated fragment and the basis set employed.

In the approach used here, relativistic effects are taken into account in two steps, both based on the Douglas–Kroll Hamiltonian.¹⁰ In the first step, scalar relativistic effects are already taken into account in the basis set generation. Next, spin-free eigenstates are obtained in the Complete Active Space Self-Consistent Field (CASSCF) method,¹¹ as implemented in MOLCAS 7.6.¹² The active space of CASSCF included nine electrons spanning seven 4f orbitals of the Dy³⁺ ion. In the second step, spin–orbit coupling is taken into account within the space of calculated spin-free eigenstates using the RASSI module.¹³ The obtained spin–orbit multiplets, corresponding to exact electronic states of the complex, were used for the calculation of matrix elements of the magnetic moment. The latter were employed in the module SINGLE_ANISO^{12b} which computed the magnetic properties and parameters of the Zeeman Hamiltonian of the fragments. This method has been previously applied for the elucidation of electronic and magnetic properties of other lanthanide complexes.^{1a,7,8,14}

The results of calculations on mononuclear Dy fragments do not differ significantly for the two structural and two basis set

Received: September 17, 2012

Published: October 30, 2012

approximations (Table S2). The convergence of the energies of CASSCF terms in the series of calculations A1–B2 (Table S1), corresponding to a gradual increase of the orbital basis set, allows us to conclude that the CASSCF wave functions obtained for the highest approximation (B2) have the correct form. The latter is generally not guaranteed because of a complex self-consistency procedure employed in CASSCF calculations, which increases the risk of convergence to incorrect wave functions when the basis set or the space of active orbitals is increased.¹² Following the convergence of terms and multiplet energies, the calculated g tensors for the lowest eight Kramers doublets (KDs) on the Dy site also show clear convergence in the series of A1–B2 approximations (Table S3). Given the high sensitivity of the g tensors of lanthanide complexes to the computational approximation,^{1a,7,8} this convergence gives us confidence that the latter are reproduced quite accurately in our highest approximation B2.

Table 1 shows the results for the lowest KDs on the Dy center obtained in the highest computational approximation.

Table 1. Energies of the Lowest Kramers Doublet of Each Dy Center in the Dy₆ Molecule

KD	E (cm ⁻¹)	KD	E (cm ⁻¹)
1	0.0	5	237.2
2	56.0	6	252.5
3	113.8	7	343.2
4	174.3	8	477.2

g tensor of the ground KD:

$$g_x = 0.18; g_y = 0.53; g_z = 19.26$$

We can see that the first excited KD is separated from the ground one by a gap which is much larger than the expected exchange splitting in this complex, which means that only the magnetic interactions between the ground KDs on the Dy ions was relevant. The g tensor of the ground KD of individual Dy centers, although being axial, contains relatively large transverse components (g_x and g_y) which means that the blockage of magnetization at individual Dy ions will not be achieved due to fast intra-ionic quantum tunneling of magnetization. This conclusion is in line with the experimental observation that, although displaying slow magnetic relaxation, the Dy₆ molecule does not show blocking of the magnetization until $T = 2$ K.⁹

The directions of local anisotropy axes on the Dy sites (corresponding to g_z in Table 1), calculated in the approximation B2, are shown in Figure 1 by dashed lines. The angle of these axes with the main symmetry axis of the complex (S_6) is 43°. The angle between anisotropy axes on neighboring Dy sites is 73°. Table S4 shows that these angles achieve convergence in the series of employed approximations.

The exchange interaction between nearest-neighbor Dy sites was simulated within the Lines model as in our previous work,^{1a,7,8,14} using one phenomenological parameter. The intramolecular dipole–dipole interactions between the local magnetic moments of all Dy ions were included. The calculations of the exchange spectrum and of the magnetic properties have been performed with the program POLY_ANISO.¹⁵ Because of the strong axiality of the KDs on the Dy sites (Table 1), the resulting magnetic interaction between the sites (exchange + dipolar) is described in a good approximation by a non-collinear Ising model:

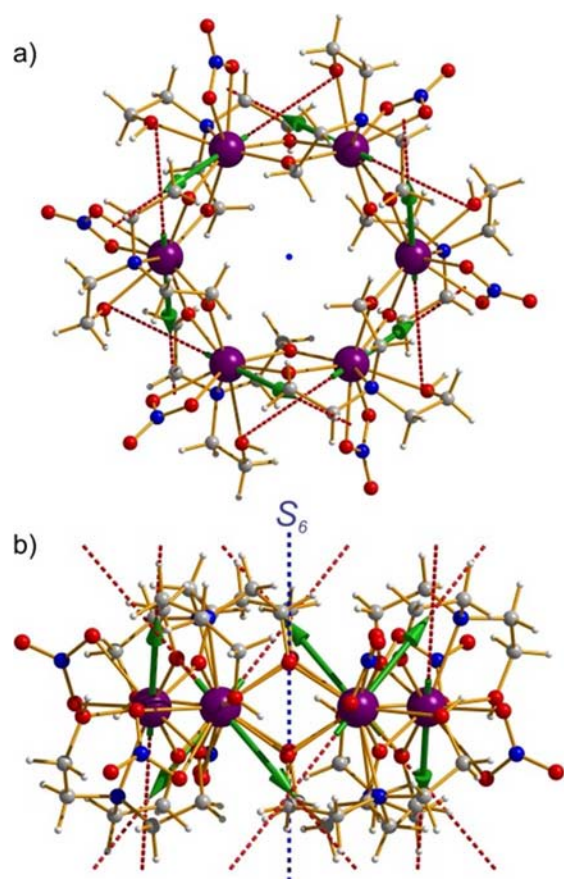


Figure 1. Orientations of the local anisotropy axes in the ground Kramers doublet on the Dy sites (red dashed lines) and of the local magnetic moments in the ground exchange doublet of the Dy₆ complex (green arrows). The S_6 improper rotation axis is shown in blue as a dot in (a), and as a dashed line in (b).

$$\hat{H} = - \sum_{i=1}^6 J_{i,z}^{\text{exch}} \tilde{s}_{i,z} \tilde{s}_{(i+1),z} - \sum_{i=1}^6 \sum_{j>i}^6 J_{i,j}^{\text{dipolar}} \tilde{s}_{i,z} \tilde{s}_{j,z} \quad (1)$$

where \tilde{s}_{ij} is the projection of the pseudospin $\tilde{s} = 1/2$ characterizing the KD of the site Dy_{*i*} on the corresponding local magnetic axis (z); J^{exch} are the exchange coupling constants between nearest neighbor Dy sites and J_{ij}^{dipolar} are dipolar magnetic interaction constants between centers i and j . The dipolar interaction is taken into account exactly, since all the information needed for its calculation is available from *ab initio* calculations.

Table 2 shows the dipolar interaction constants between all Dy ions calculated *ab initio* in the highest approximation. We can see that the dipolar interaction between all pairs of metal ions is antiferromagnetic, while the dipolar interaction between opposite Dy centers is stronger than the interaction between next-nearest neighbors (for calculations in other approximations see Table S5). This is due to the fact that the anisotropy

Table 2. Calculated Constants of the Dipolar Interaction (cm⁻¹) between the Ground Kramers Doublets of Different Magnetic Centers in Dy₆

nearest neighbor ^a	next-nearest neighbor ^a	opposite ^a
-4.168	-0.196	-0.387

^aSee Figure 2.

axes on opposite Dy centers are parallel, thus maximizing the value of the dipolar interaction, while the magnetic moments of next-nearest neighbors make an angle of 73° , which significantly lowers the magnitude of the dipolar interaction. As a result of antiferromagnetic dipolar coupling and of the S_6 symmetry of the complex, local magnetic moments on Dy centers completely compensate each other in the ground exchange state, and the Dy_6 molecule shows no magnetic moment (see Table 3 and Figure 1).

Table 3. Lowest Exchange Doublets (cm^{-1}) Arising from the Dipolar Coupling, the Corresponding Tunnel Splitting (Δ_{tun}), and the g_z Value of Each Doublet (g_x and $g_y = 0$)

no.	E (cm^{-1})	Δ_{tun}	g_z
1	0.00000000	0.00E+00	0.0
	0.00000000		
2	4.389426111	9.47×10^{-6}	0.0
	4.389435587		
3	4.390119911	0.00E+00	0.0
	4.390119911		
4	4.390125127	0.00E+00	1.1
	4.390125127		
5	4.391775363	0.00E+00	1.2
	4.391775363		
6	4.391781618	0.00E+00	1.1
	4.391781618		
7	4.393218925	1.08×10^{-5}	1.2
	4.393229768		
8	4.612801449	1.41×10^{-3}	0.0
	4.614214440		
9	4.614214440	2.58×10^{-3}	23.0
	4.616800664		
10	4.617088144	0.00E+00	0.0
	4.617088144		

As can be seen in Figure 1a, the magnetic moments of the Dy ions have a toroidal component, projected onto the plane of the wheel. This situation is very similar to the toroidal ground state of previously investigated Dy_3 triangles.³ The difference between the Dy_3 triangles and the present Dy_6 molecule is that the three magnetic moments of the Dy ions in the Dy_3 triangles do not compensate completely (in the ground state they sum up into a residual magnetic moment $\mu_z = 0.56 \mu_B$ oriented perpendicular to the plane of the three Dy atoms), because of a lack of symmetry in the complex. Thus the high symmetry of Dy_6 is a crucial condition for its non-magnetic ground state. Moreover, the lowest excited exchange states are also non-magnetic. The quantum tunneling in the low-lying exchange doublets is expected to be weak (the tunneling gaps in Table 3 are relatively small) and will not contribute alone to magnetic relaxation. However, these states are related to each other by the reversal of the moment of one single Dy ion, a process which will not be slow given the relatively large transversal g factors of the Dy ions (see Table 1). Furthermore, Table 3 shows that they are very close in energy implying fast relaxation of magnetization through this bunch of excited exchange states. This precludes the blocking of magnetization in Dy_6 at low temperatures without an applied dc field, as evidenced in the lack of a maximum in the experimental out-of-phase ($\chi_M''(\omega)$) ac magnetic susceptibility.⁹

We stress, however, that the obtained results do not preclude the blocking of the *toroidal magnetization* at low temperatures.

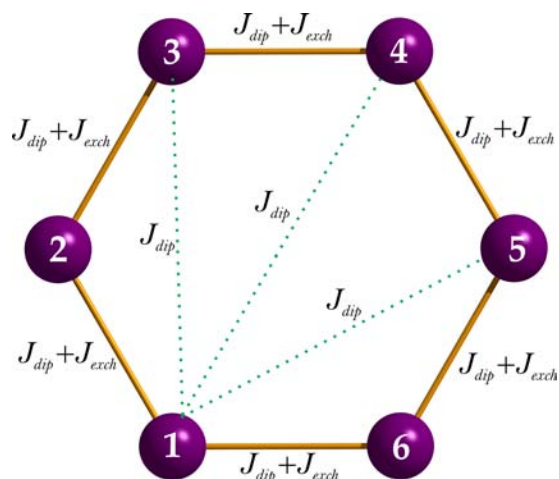


Figure 2. Magnetic interactions between Dy ions in the Dy_6 complex. Dipolar coupling is non-negligible for all pairs of metal ions (shown completely for center 1), while exchange interactions are only important for nearest-neighbor ions.

Indeed, the ground doublet, which possesses a net toroidal moment, is characterized by a negligible tunneling gap. For temperatures significantly lower than the energy gap separating these doublets from the ground state (ca. 4.4 cm^{-1}) the toroidal magnetic moment of the complex will be completely blocked. This blocking, however, cannot be evidenced via ac magnetic susceptibility or recovery magnetization measurements due to the lack of dipolar magnetic moment in the ground state. A suitable technique would be NMR which could probe the magnetic dynamics on individual Dy sites, through the broadening of ^{13}C NMR lines, for example.¹⁶

On the basis of the calculated $2^6 = 64$ exchange eigenstates and local excited states on Dy ions, we have computed the magnetic properties of the Dy_6 molecule using the package POLY_ANISO interfaced with MOLCAS.¹⁵ Setting $J_{i,i+1}^{\text{exch}} = 0$ and taking into account only the intramolecular dipolar interaction, we obtain a reasonable description of the magnetic properties (Figure 3). This supports the correctness of the calculated exchange states in Table 3 and their magnetic properties, and points toward the relative weakness of exchange parameters J_{exch} , which is usually the case in polynuclear complexes containing only lanthanide ions.¹⁷ Since the dipolar interaction was taken into account exactly, our approach did not involve any fitting parameters. Figure 4 displays the evolution of the lowest exchange coupled states in an applied magnetic field. As one can see, the ground state is non-magnetic in zero applied field, while the level crossing takes place upon application of a field of $\sim 0.65 \text{ T}$.

The obtained toroidal magnetic moment in the present Dy_6 complex could be, in principle, increased by forcing the local anisotropy axes of the Dy ions to lie in the plane of the molecule. Theoretically, this goal can be achieved by modifying the ligand environment on the Dy sites. Furthermore, such an arrangement of the local anisotropy axes would lead to much stronger dipolar coupling between neighboring centers increasing significantly the stabilization energy of the toroidal state. In contrast to the present Dy_6 molecule, the stabilization energy of the toroidal moment in the recently investigated Dy_4 compound⁸ is already at its highest limit, because the magnetic moments of the four Dy ions lie almost in the plane of the molecule.

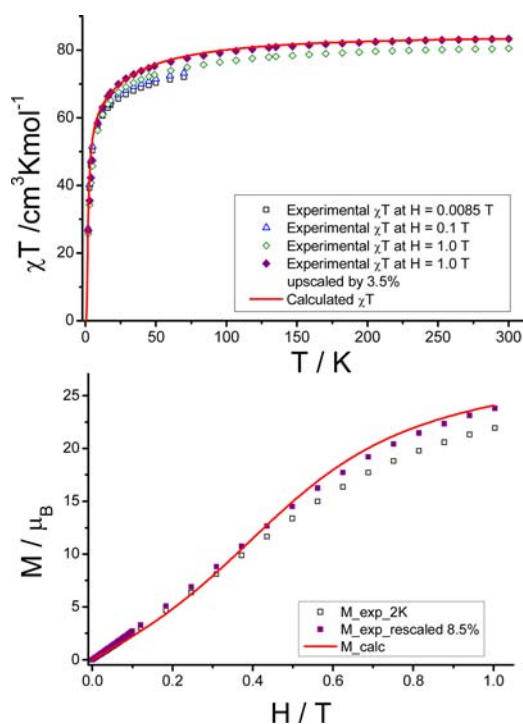


Figure 3. (top) Comparison between the measured and calculated magnetic susceptibility of the Dy_6 complex. (bottom) Molar magnetization at $T = 2.0$ K. Up-scaling of the experimental data was performed only to estimate the difference.

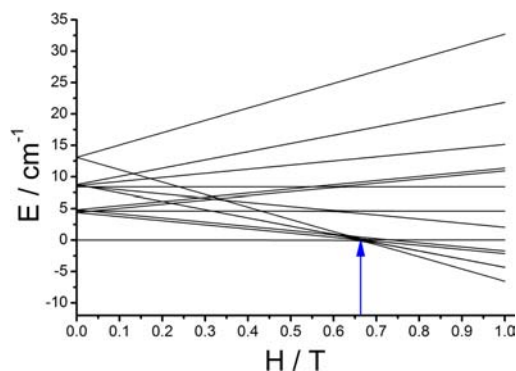


Figure 4. Evolution of the exchange states in an applied magnetic field along the main symmetry axis of the Dy_6 complex. The blue arrow shows the magnetic field where the ground state becomes magnetic.

In conclusion, a detailed *ab initio* investigation of the electronic and magnetic structure of the Dy_6 wheel revealed a non-magnetic ground state with a net toroidal magnetic moment. This arises due to the high symmetry of the wheel and the dipolar interactions of Dy magnetic moments in the molecule, which are large enough to stabilize this state with respect to the magnetic ones by ca. 4.4 cm^{-1} . The obtained strong stabilization of toroidal magnetic moment allows for its experimental observation.

■ ASSOCIATED CONTENT

📄 Supporting Information

Details of fragment *ab initio* calculation of the magnetic properties of individual Dy sites; calculated low-lying spectrum of magnetic states of Dy_6 . This material is available free of charge via the Internet at <http://pubs.acs.org>.

■ AUTHOR INFORMATION

Corresponding Author

Liviu.Ungur@chem.kuleuven.be; Liviu.Chibotaru@chem.kuleuven.be

Notes

The authors declare no competing financial interest.

■ ACKNOWLEDGMENTS

L.U. is a postdoc of the Fonds Wetenschappelijk Onderzoek–Vlaanderen and also gratefully acknowledges the research grant Methusalem from K.U. Leuven. K.S.M. acknowledges the receipt of Australian Research Council Discovery and LIEF grants for this work. E.K.B. thanks the EPSRC.

■ REFERENCES

- (1) (a) Chibotaru, L. F.; Ungur, L.; Soncini, A. *Angew. Chem., Int. Ed.* **2008**, *47*, 4126. (b) Luzon, J.; Bernot, K.; Hewitt, I. J.; Anson, C. E.; Powell, A. K.; Sessoli, R. *Phys. Rev. Lett.* **2008**, *100*, 247205.
- (2) (a) Schmidt, H. *J. Phys.: Condens. Matter* **2008**, *47*, 434201. (b) Kaelberer, T.; Fedotov, V. A.; Papisimakis, N.; Tsai, D. P.; Zheludev, N. I. *Science* **2010**, *330*, 1510. (c) Plokhov, D. I.; Zvezdin, A. K.; Popov, A. I. *Phys. Rev. B* **2011**, *83*, 184415.
- (3) Soncini, A.; Chibotaru, L. F. *Phys. Rev. B* **2008**, *77*, 220406.
- (4) (a) Plokhov, D. I.; Popov, A. I.; Zvezdin, A. K. *Phys. Rev. B* **2011**, *84*, 224436. (b) Soncini, A.; Chibotaru, L. F. *Phys. Rev. B* **2010**, *81*, 132403.
- (5) Dubovik, V. M.; Tosunyan, L. A.; Tugushev, V. V. *JETP* **1986**, *63*, 344. Marinov, K.; Boardman, A. D.; Fedotov, V. A.; Zheludev, N. *New J. Phys.* **2007**, *9*, 324.
- (6) Popov, A. I.; Plokhov, D. I.; Zvezdin, A. K. *EPL* **2009**, *87*, 67004. Trif, M.; Troiani, F.; Stepanenko, D.; Loss, D. *Phys. Rev. Lett.* **2008**, *101*, 217201.
- (7) Novitchi, Gh.; Pilet, G.; Ungur, L.; Moshchalkov, V. V.; Wernsdorfer, W.; Chibotaru, L. F.; Luneau, D.; Powell, A. K. *Chem. Sci.* **2012**, *3*, 1169.
- (8) Guo, P.-H.; Liu, J.-L.; Zhang, Z.-M.; Ungur, L.; Chibotaru, L. F.; Leng, J.-D.; Guo, F.-S.; Tong, M.-L. *Inorg. Chem.* **2012**, *51*, 1233.
- (9) Langley, S. K.; Moubaraki, B.; Forsyth, C. M.; Gass, I. A.; Murray, K. S. *Dalton Trans.* **2010**, *39*, 1705.
- (10) Hess, B. A.; Maarian, C. M.; Wahlgren, U.; Gropen, O. *Chem. Phys. Lett.* **1996**, *251*, 365.
- (11) Roos, B. O.; Malmqvist, P. Å. *Phys. Chem. Chem. Phys.* **2004**, *6*, 2919.
- (12) (a) Aquilante, F.; De Vico, L.; Ferre, N.; Ghigo, G.; Malmqvist, P. Å.; Neogady, P.; Pedersen, T. B.; Pitonak, M.; Reiher, M.; Roos, B. O.; Serrano-Andres, L.; Urban, M.; Veryazov, V.; Lindh, R. *J. Comput. Chem.* **2010**, *31*, 224. (b) For SINGLE_ANISO module, see: <http://www.molcas.org/documentation/manual/node95.html>.
- (13) Malmqvist, P. Å.; Roos, B. O.; Schimmelpfennig, B. *Chem. Phys. Lett.* **2002**, *357*, 230.
- (14) Langley, S. K.; Ungur, L.; Chilton, N. F.; Moubaraki, B.; Chibotaru, L. F.; Murray, K. S. *Chem. Eur. J.* **2011**, *17*, 9209.
- (15) Chibotaru, L. F.; Ungur, L., Program POLY_ANISO, University of Leuven, 2006.
- (16) Gossuin, Y.; Hocq, A.; Vuong, Q. L.; Disch, S.; Hermann, R. P.; Gillis, P. *Nanotechnology* **2008**, *19*, 475102.
- (17) (a) Tuna, F.; Smith, C. A.; Bodensteiner, M.; Ungur, L.; Chibotaru, L. F.; McInnes, E. J. L.; Winpenny, R. E. P.; Collison, D.; Layfield, R. A. *Angew. Chem., Int. Ed.* **2012**, *51*, 6976. (b) Cañadillas-Delgado, L.; Fabelo, O.; Cano, J.; Pasán, J.; Delgado, F. S.; Lloret, F.; Julve, M.; Ruiz-Pérez, C. *CrystEngComm* **2009**, *11*, 2131. (c) John, D.; Rohde, A.; Urland, W. *Z. Naturforsch.* **2006**, *61b*, 699.